J Electr Eng Technol Vol. 9, No. 2: 609-614, 2014
http://dx.doi.org/10.5370/JEET.2014.9.2.609

ISSN(Print) 1975-0102
ISSN(Online) 2093-7423

Effects of an Aluminum Contact on the Carrier Mobility and Threshold Voltage of Zinc Tin Oxide Transparent Thin Film Transistors

Tae-Young Ma†

Abstract – We fabricated amorphous zinc tin oxide (ZTO) transparent thin-film transistors (TTFTs). The effects of Al electrode on the mobility and threshold voltage of the ZTO TTFTs were investigated. It was found that the aluminum (Al)-ZTO contact decreased the mobility and increased the threshold voltage. Traps, originating from AlO_x, were assumed to be the cause of degradation. An indium tin oxide film was inserted between Al and ZTO as a buffer layer, forming an ohmic contact, which was revealed to improve the performance of ZTO TTFTs.

Keywords: Zinc tin oxide, Transparent thin film transistors, Aluminium contact, Ohmic contact

1. Introduction

Considerable improvement in the performance of transparent thin-film transistors (TTFTs) has been achieved using amorphous oxide semiconductors (AOSs) as active layers in TTFTs [1-3]. Amorphous films have a smoother surface than polycrystalline films. Furthermore, post-transition metal cations contained in AOSs generate extraneous conduction paths in the crystal structure via the overlap of spherically spread metal ns orbitals (n is the principal quantum number), which can yield high electron mobility in AOS TTFTs [4].

Thus far, the most widely studied topics related to AOS TTFTs have been mobility improvement [5, 6] and bias stability [7, 8]. It was assumed that the gate dielectric-AOS interface influences both the carrier mobility and the bias stability. However, the contact properties between the AOS and the source/drain electrodes are also important factors in the advancement of AOS TTFTs.

A variety of metals such as Al [9], In [10], and Au/Ti [11] have been used as source/drain electrodes for AOS TTFTs. Among them, Al is the most desirable electrode because of its extremely low resistivity, good adhesion, and weldability. On the other hand, it is also known that Al is easily oxidized when exposed to air. Because of the high oxygen affinity of Al, an AlO_x layer will be formed at the Al-AOS interface as AOSs contain a considerable amount of oxygen, which might reduce the quality of AOS TTFTs.

In this study, we fabricated TTFTs using amorphous zinc tin oxide as an active layer. The zinc tin oxide (ZTO) film was thought to be an effective active layer for TTFTs because of its wide energy band gap and high resistivity [12-14]. We have reported that ZTO TTFTs employing In as source/drain electrodes exhibit a mobility greater than 18.0 cm^2/Vs [15]. Indium is known to be ohmic when combined with zinc-base oxide [10]. Although indium is known to be ohmic with zinc-base oxide, it has limited practical applications, because of its ease of scratching and low melting point. Alternatively, we adopted Al as the source / drain electrode for ZTO TTFTs. Mobility deterioration in ZTO TTFTs with Al electrodes was observed. Thus, we deposited a transparent indium tin oxide (ITO) conductor between Al electrodes and ZTO as a buffer layer. We could improve the mobility of ZTO TTFTs successfully by the ITO buffer layer.

2. Experimental Procedure

Heavily doped n-type Si wafers, acting as gate electrodes, were thermally oxidized. An Al_2O_3 film was sequentially grown by atomic layer deposition to form a gate dielectric layer. The thicknesses of SiO_2 and Al_2O_3 were 120 nm and 30 nm, respectively. A 40-nm-thick ZTO film was deposited on the wafer using RF magnetron sputtering. A 3-in zinc tin oxide (Zn : Sn = 3:2) target, purchased from Aldrich, was sputtered in oxygen-mixed argon [$O_2/(Ar + O_2) = 40\%$] at 0.66 Pa and 70 W. The substrate temperature was maintained at 300 °C during ZTO deposition. Next, the ZTO-coated wafer was rapidly annealed at 400 °C for 5 min. A section of the dielectric film was etched to expose the surface of the heavily doped Si wafer. Finally, 600-nm-thick In or 300-nm-thick Al was deposited on the ZTO films as the source, drain, and gate electrodes of the ZTO TTFTs. Alternatively, 20-nm-thick ITO was deposited on the ZTO films before Al deposition to act as a buffer layer. RF magnetron sputtering was carried out at 0.66 Pa and 100 W to deposit ITO. The channel length and width defined by the stainless steel masks were 400 and 500 μm, respectively.

The crystallographic properties of ZTO films were studied by X-ray diffraction with CuKα (λ = 1.5406 Å) radiation, where 2θ = 20°–60°. The drain current (I_D) as a

† Corresponding Author: Dept. of Electrical Engineering, Gyeongsang National University, Korea. (tyma@gnu.ac.kr)
Received: November 28, 2012; Accepted: May 27, 2013

function of both the drain-source voltage (V_{DS}) and the gate-source voltage (V_{GS}) was measured in the dark using a semiconductor parameter analyzer (Keithley 4200). We derived the threshold voltage (V_{TH}) using a linear extrapolation of the $I_D^{1/2}$-V_{GS} curve [16] and derived the mobility (μ_{SAT}) using the slope of the $I_D^{1/2}$-V_{GS} curve [17].

3. Results and Discussion

We examined the crystalline structure of ZTO used as an active layer. Fig. 1 shows the XRD results for 250-nm-thick ZTO films, both as-deposited and annealed at 400 °C for 30 min. Both the ZTO films showed a broad peak that appears to be a combination of a broad ZnO (002) peak and a SnO_2 (110) peak, confirming that the ZTO films were in an amorphous state.

It is well known that a high contact resistance between the source/drain and the channel layer reduces the voltage drop across the channel, which aggravates the device performance of TFTs [18-20]. First, we metalized ZTO TTFTs with In to create source/drain electrodes [ZTO TTFT(In)]. Fig. 2 shows the output characteristics of the ZTO TTFT(In). The typical output characteristics of TFTs with a good saturation were obtained. Second, ZTO TTFTs with Al source/drain electrodes [ZTO TTFT(Al)] were fabricated so that their characteristics could be compared with those of ZTO TTFT(In). The transfer characteristics [log (I_D)-V_{GS} and $I_D^{1/2}$-V_{GS}] of ZTO TTFT(Al) and ZTO TTFT(In) at a drain-source voltage (V_{DS}) = 15 V are shown in Fig. 3. Mobility μ_{SAT}, threshold voltage V_{TH}, and on/off current ratio (I_{ON}/I_{OFF}) of ZTO TTFT(In) were 17.4 cm^2/Vs, 2.5 V, and $>10^7$, respectively. A decrease in μ_{SAT} and an increase in V_{TH} were found for ZTO TTFT(Al), relative to ZTO TTFT(In). The μ_{SAT}, V_{TH}, and I_{ON}/I_{OFF} of ZTO TTFT(Al) were 12.7 cm^2/Vs, 5.0 V, and $>10^7$, respectively. Many research groups [18-20] have reported that the current retarding factors existed at the metal electrode-AOS active layer interface adversely affects the properties of TTFTs. A potential barrier, which restricts electron injection from the metal electrode into the active layer, can be formed at the metal-semiconductor interface. The potential barrier height (ϕ_B) is determined by the difference between the work function potential of the metal (ϕ_m) and χ of the semiconductor, where $q\chi$ is the electron affinity. When $\phi_m > \chi$ in an n-type semiconductor, a rectifying contact is created. The electron affinity of ZnO [21] and SnO_2 [22] has been reported to be dependent on the material conditions: electron density, crystal structure, surface state, etc. Because electron affinity measurement is beyond the scope of our research, we cannot estimate the ϕ_B variation with metal contact. From the mobility degradation in ZTO TTFT(Al), however, it is clear that current-retarding factors are created at the Al-ZTO contact. If the Al-ZTO contact is a rectifying contact, either the source-channel junction or the channel-drain junction will be reverse biased. Electrons are transported across a metal-semiconductor junction under reverse bias in the following ways [23-25]: thermal generation (I_{GE}) in a space charge layer, field emission (I_{FE}) or thermionic field emission (I_{TFE}) through the potential barrier, and thermionic emission (I_{TE}) over the potential barrier.

The thermionic emission current I_{TE} of the Schottky barrier is negligible in the reverse bias mode. Accordingly, I_{GE}, I_{FE}, or I_{TFE} is the dominant current at the reverse-biased metal-semiconductor contact. The trap-assisted thermal generation current I_{GE} is proportional to $(1 + V_R/V_{bi})^{1/2}$ [23],

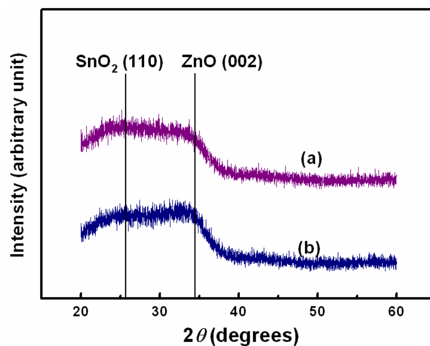

Fig. 1. XRD spectra of ZTO films: (a) as-deposited and (b) annealed at 400 °C.

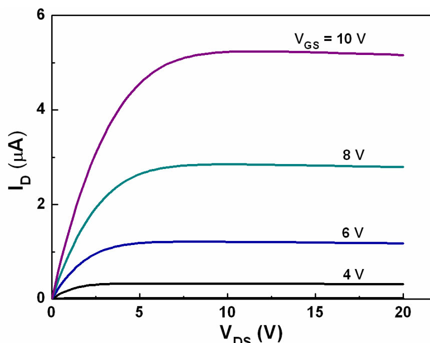

Fig. 2. Output characteristics [I_D versus V_{DS}] of ZTO TTFT(In) using In as the source/drain electrode with W/L = 500 μm/400 μm.

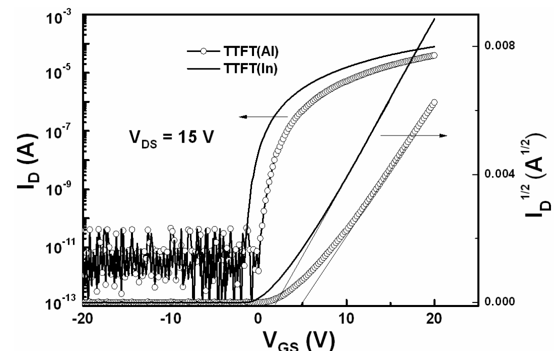

Fig. 3. Transfer characteristics [log I_D versus V_{GS} and $I_D^{1/2}$ versus V_{GS}] of ZTO TTFT(In) and ZTO TTFT(Al).

where V_R and V_{bi} are the voltage drop across the Schottky barrier and the built-in potential of the Schottky contact, respectively. The field emission current and thermionic field emission current are known to be exponentially proportional to V_R such that $I_{FE} \propto V_R^2 \exp(-K_1/qV_R)$ [24] and $I_{TFE} \propto \exp(qV_R/K_2)$ [25], where K_1 and K_2 are the characteristic energies of the field emission current and thermionic field emission current, respectively. The drain-source voltage V_{DS} is divided between the two Schottky contacts and the channel. The source-channel contact is reverse biased, and the drain-channel contact is forward biased. Thus, V_R in the current relations can be replaced by V_{DS} if $V_{DS} < (V_{GS} - V_{TH})$. Fig. 4 shows I_D versus $V_{DS}^{1/2}$ curves for the ZTO TTFT(Al). The linearity of the curve indicates that the thermal generation current I_{GE} is dominant in the Al-ZTO contact. No evidences of the field emissions were observed through the curve fittings of the output characteristics of the ZTO TTFT(Al). To further study the Al-ZTO interface, we intentionally annealed the ZTO TTFT(Al) at 400 °C for 5 min in air. We assumed that annealing creates more traps at the Al-ZTO interface by generating more incomplete Al-oxygen bonds. The transfer characteristic of the annealed ZTO TTFT(Al) is shown in Fig. 5. The threshold voltage V_{TH} of the annealed ZTO TFT(Al) shifted toward a negative direction . It is known that the neutralized positive charges by trapping electrons in the gate dielectric shift V_{TH} toward a positive direction [26].

We think that some of the neutralized positive charges detrap electrons during the annealing process, and the revived positive charges may be the cause of the negative V_{TH} shift of the annealed ZTO TFT(Al). It was found that the V_{TH} of the annealed ZTO TFT(Al) increased by repeating measurements. The mobility μ_{SAT} of the annealed ZTO TFT(Al) decreased to 2.5 cm^2/Vs. The output characteristics of the ZTO TTFT(Al) before and after annealing are compared in Fig. 6. A significant difference in the trend of the curve is observed, which means that changes in the conduction mechanism at the Al-ZTO interface occurred by the annealing process. The output characteristic curves of the annealed ZTO TTFT(Al) show the general form of parabola, i.e. $I_D \propto V_{DS}^2$. This square-law dependence was found at the space-charge-limited current (I_{SCL}) flow from source to drain after punch-through [27]. Richman [27] induced I_{SCL} resulting from the injection of electron from the source as

$$I_{SCL} = 9\varepsilon_s\mu_n AV^2 / 8L^3 \qquad (1)$$

where, ε_s is the permittivity of ZTO, μ_n is the electron mobility, A is the area of the depletion region, V is the voltage applied at the depletion region, and L is the length of the depletion region. The transformed curves [$I_D^{1/2}$ versus V_{DS}] of the annealed ZTO TTFT(Al) are shown in Fig. 7.

The linearity found in Fig. 7 indicates that I_{SCL} is a dominant constituent of I_D when $V_{DS} < (V_{GS} - V_{TH})$. It was reported that the square-law dependence of V_{DS} on I_D is evident where the injected carrier density is greater than the background concentration of thermally generated carriers in the depletion region [27]. The increased traps at

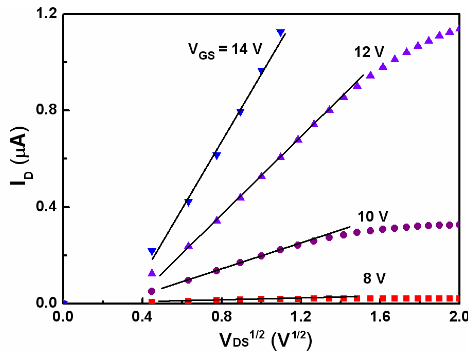

Fig. 4. I_D versus $V_{DS}^{1/2}$ of ZTO TTFT(Al). The linearity means that the thermal generation current is dominant when $V_{DS} > (V_{GS} - V_{TH})$.

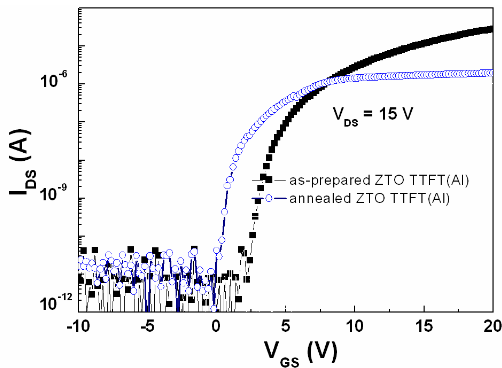

Fig. 5. Transfer characteristic of the ZTO TTFT(Al) annealed at 400 °C for 5 min. Transfer characteristic of the as-prepared ZTO TTFT(Al) are presented for comparison.

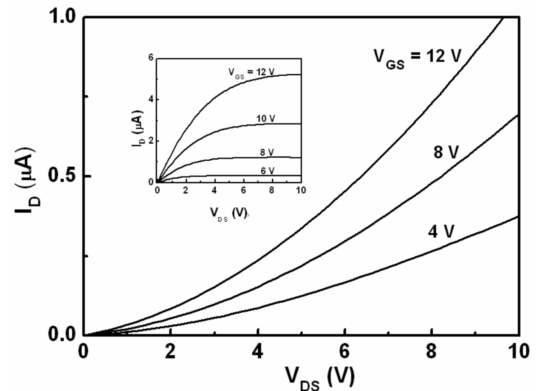

Fig. 6. Output characteristic of the ZTO TTFT(Al) annealed at 400 °C for 5 min. The inset shows the output characteristic of the as-prepared ZTO TTFT(Al).

the Al/ZTO interface by the annealing process capture electrons in the channel, which expands the depletion region into the channel. It is considered that the electrons captured by the traps are easily injected into the depletion region, which is the source for I_{SCL}. The space-charge-limited current through the depletion region at the reverse-biased source-channel interface dominates I_D. The length of the depletion region L was estimated from Eq. (1) by substituting the measured I_D and V_{DS} [Fig. 7] for I_{SCL} and V. The field-effect mobility μ_n of the annealed ZTO TTFT(Al) (0.3 cm^2/Vsec) was extracted from Fig. 5. Fig. 8 shows the calculated L as a function of V_{GS}. The L is found to be decreased with V_{GS}, which is due to the increased channel conductivity [28]. The obtained L is shown to be 0.8 ~2.2 μm which is too thick to be tunneled. The depletion length at a p^+-n junction is inversely proportional to the donor density (N_D) [29]. The L of 0.8 ~ 2.2 μm corresponds to $N_D \approx 1.9 \times 10^{15} \sim 0.7 \times 10^{15}$ cm^{-3} when being estimated from the p^+-n junction. On the basis of the above observation, we concluded that the Al-ZTO contact is rectifying, and the AlO_x layer exists at the Al-ZTO interface. The incomplete bonds in the AlO_x layer act as traps, i.e., scattering centers, which are the cause of the mobility degradation in the ZTO TTFT(Al). The traps are negatively charged by electron occupation, which increases the potential barrier height at the Al-ZTO contact, resulting in a high threshold voltage comparing with the In-ZTO contact.

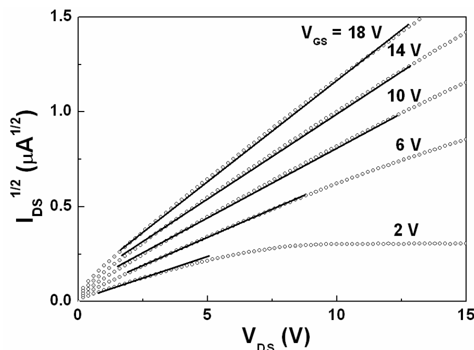

Fig. 7. The transformed curve [$I_D^{1/2}$ versus V_{DS}] of the ZTO TTFT(Al) annealed at 400 °C for 5 min.

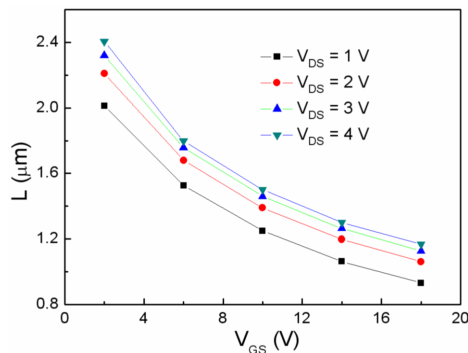

Fig. 8. The calculated length of the depletion region as a function of V_{GS}.

The potential barrier width at the metal-semiconductor contact is proportional to the carrier density of the semiconductor. Commonly, the active region under the source/drain electrodes is heavily doped prior to metal deposition, so as to eliminate the contact resistance. The degenerated semiconductor narrows the width of the potential barrier, and electrons penetrate the thin potential barrier. This tunneling effect neutralizes the potential barrier that obstructs the flow of electrons between the channel and the source/drain electrodes. High-resistivity AOS films are used to create the active layer of the TTFT to suppress the leakage current through the channel. It is difficult to dope the AOS films for source/drain contact. Accordingly, we coated a highly conductive ITO film as a buffer layer between the Al electrodes and the ZTO film so as to reduce the source/drain contact resistance to I_D. The schematic diagram and transfer characteristic of the TTFT adopting ITO as a buffer layer [ZTO TTFT(ITO)] are shown in Fig. 9(a) and (b), respectively. The measured μ_{SAT}, V_{TH}, and I_{ON}/I_{OFF} of the ZTO TTFT(ITO) were 20.3 cm^2/Vs, 4.0 V, and >10^7, respectively. It was found that the ITO buffer layer effectively eliminated the contact resistance at the Al-ZTO contact, which confirms that the highly conductive ITO film plays the role of the degenerated layer between electrodes and semiconductor films narrowing the width of the potential [30]. The annealing at 400 °C for 5 min degraded μ_{SAT} of the ZTO TTFT(ITO) to 15.2 cm^2/Vs which was recovered to its original value a day later.

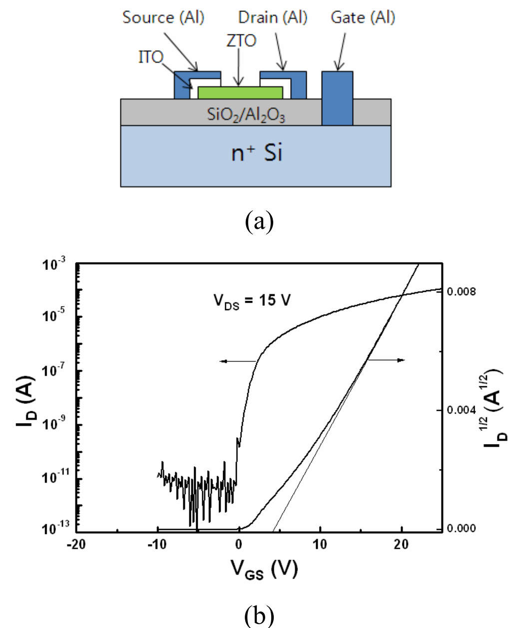

Fig. 9. (a) Schematic diagram and (b) Transfer characteristics [log I_D versus V_{GS} and $I_D^{1/2}$ versus V_{GS}] of ZTO TTFT(ITO). Indium tin oxide was inserted between Al and ZTO as a buffer layer to improve the contact properties.

4. Conclusion

We fabricated ZTO TTFTs using Al and In as source/drain electrodes. A decrease in mobility and an increase in threshold voltage were observed when Al was employed as an electrode, compared to the case when In was used as an electrode. The traps created by the incomplete bonds at the Al-ZTO contact can reduce the carrier mobility of the ZTO TTFT(Al), and the negatively charged traps (caused by electron occupation) can increase the potential barrier height at the Al-ZTO contact, resulting in a high threshold voltage. We inserted a highly conductive ITO film as a buffer layer between the Al electrodes and the ZTO film. This buffer layer ITO enhanced the mobility to 20.3 cm^2/Vs and lowered the threshold voltage to 4.0 V.

Acknowledgements

This research was supported by Basic Science Research Program through the National Research Foundation of Korea(NRF) funded by the Ministry of Education, Science and Technology(2010-0007697).

References

[1] N. L. Dehuff, E. S. Kettenring, D. Hong, H. Q. Chiang, J. F. Wager, R. L. Hoffman, C.-H. Park, and D. A. Keszler, "Transparent thin-film transistors with zinc indium oxide channel layer," J. Appl. Phys., Vol. 97, pp. 064505, 2005.

[2] J. Liu, D. B. Buchholz, J. W. Hennek, R. Chang, A. Facchetti, and T. J. Marks, "All-Amorphous-Oxide Transparent, Flexible Thin-Film Transistors. Efficacy of Bilayer Gate Dielectrics," J. Am. Chem. Soc., Vol. 132, pp. 11934-11942, 2010.

[3] A. Dey, D. R. Allee, and L. T. Clark, "Impact of drain bias stress on forward/reverse mode operation of amorphous ZIO TFTs," Solid State Electron., Vol. 62, pp. 19-24, 2011.

[4] K. Nomura, H. Ohta, A. Takagi, T. Kamiya, M. Hirano, and H. Hosono, "Room-temperature fabric-cation of transparent flexible thin-film transistors using amorphous oxide semiconductors," Nature, Vol. 432, pp. 488-492, 2003.

[5] Z. Yuan, X. Zhu, X. Wang, X. Cai, B. Zhang, D. Qiu, and H. Wu, "Annealing effects of In_2O_3 thin films on electrical properties and application in thin film transistors," Thin Solid Films, Vol. 519, pp. 3254-3258, 2011.

[6] J. S. Park, W. Maeng, H. Kim, and J. Park, "Review of recent developments in amorphous oxide semi-conductor thin-film transistor devices," Thin Solid Films, Vol. 520, pp. 1679-1693, 2011.

[7] M. Fakhri, P. Gorrn, T. Weimann, P. Hinze, T. Riedl, "Enhanced stability against bias-stress of metal-oxide thin film transistors deposited at elevated tem-peratures," Applied Phys. Lett., Vol. 99, pp. 123503, 2011.

[8] M. K. Ryu, S. Yang, S. K. Park, C. Hwang, and J. K. Jeong, "Impact of Sn/Zn ratio on the gate bias and temperature-induced instability of Zn-In-Sn-O thin film transistors," Applied Phys. Lett., Vol. 95, pp. 173508, 2009.

[9] S. Lee, J. Bang, W. K., H. Uhm, and J. Park, "Effects of additive hydrogen gas on the instability due to air exposure in ZnO-based thin film transistors," Thin Solid Films, Vol. 520, pp. 1479-1483, 2011.

[10] S. Masuda, K. Kitamura, Y. Okumura, S. Miyatake, H. Tabata, and T. Kawai, "Transparent thin film transistors using ZnO as an active channel layer and their electrical properties," J. Appl. Phys., Vol. 93, pp. 1624-1630, 2003.

[11] K. Abe, N. Kaji, H. Kumomi, K. Nomura, T. Kamiya, M. Hirano, and H. Hosono, "Simple Analytical Model of On Operation of Amorphous In–Ga–Zn–O Thin-Film Transistors," IEEE Trans., Vol. ED-58, pp. 3463-3471, 2011.

[12] P. Görrn, M. Lehnhardt, T. Riedl, and W. Kowalsky, "The influence of visible light on transparent zinc tin oxide thin film transistors," Appl. Phys. Lett., Vol. 91, pp. 193504, 2007.

[13] H. Q. Chiang, J. F. Wager, R. L. Hoffman, J. Jeong, and D. A. Keszler, "High mobility transparent thin-film transistors with amorphous zinc tin oxide channel layer," Appl. Phys. Lett., Vol. 86, pp. 013503, 2005.

[14] C. N. Cha, M. H. Choi, and T. Y. Ma, "Highly transparent and resistive nanocrystalline ZnO-SnO_2 films prepared by rf magnetron sputtering," J. Electr. Eng. Technol., Vol. 7, pp. 596-560, 2012.

[15] T. Y. Ma, "The effects of oxygen partial pressure and post-annealing on the properties of ZnO-SnO_2 thin film transistors," J. KIEEME, Vol. 25, pp. 304-308, 2012.

[16] D. K. Schroder, "Semiconductor Material and Device Characterization," 1st ed., New York: A Wiley-Inter-science publication, 1990, pp. 183.

[17] D. K. Schroder, "Semiconductor Material and Device Characterization," 1st ed., New York: A Wiley-Inter-science publication, 1990, pp. 226.

[18] D. Natali, L. Fumagalli, and M. Sampietro, "Mode-ling of organic thin film transistors: Effect of contact resistances." J. Appl. Phys., Vol. 101, pp. 014501, 2007.

[19] S. Lee, H. Park, and D. C. Paine, "The effect of metallization contact resistance on the measurement of the field effect mobility of long-channel unannealed amorphous In-Zn-O thin film transistors," Thin Solid Films, Vol. 520, pp. 3769-3773, 2012.

[20] A. Ahnood, K. Ghaffarzadeh, A. Nathan, P. Servati, F. Li, M. R. Esmaeili-Rad, A. Sazonov, "Non-ohmic

contact resistance and field-effect mobility in nano-crystalline silicon thin film transistors," Appl. Phys. Lett., Vol. 93, pp. 163503, 2008.
[21] K. Jacobi, G. Zwicker, A. Gutmann, "Work function, electron affinity and band bending of zinc oxide surfaces," Surf. Sci., Vol. 141, pp. 109-125, 1984.
[22] M. N. Islam, and M. O. Hakim, "Electron affinity and work function of polycrystalline SnO_2 thin film," J. Mater. Sci. Lett., Vol. 5, pp. 63-65, 1986.
[23] W. E. Spicer, S. Eglash, I. Lindau, C. Y. Su, and P. R. Skeath, "Development and confirmation of the unified model for Schottky barrier formation and MOS interface states on III-V compounds," Thin Solid Films, Vol. 89, pp. 447-460, 1982.
[24] S. Lee, J. Park, K. Jeon, S. Kim, Y. Jeon, D. H. Kim, D. M. Kim, J. C. Park, and C. J. Kim, "Modeling and characterization of metal-semiconductor-metal-based source-drain contacts in amorphous InGaZnO thin film transistors," Appl. Phys. Lett., Vol. 96, pp. 113506, 2010.
[25] K. C. Kao, and W. Hwang, "Electrical Transport in Solid," 1st ed., New York: Pergamon Press Inc., 1981, pp. 101-110.
[26] A. K. M. Ahsan and D. K. Schroder, "Impact of post-oxidation annealing on low-frequency noise, threshold voltage, and subthreshold swing of p-channel MOSFETs," IEEE Electron Device Lett., Vol. 25, pp. 211-213, 2004.
[27] P. Richman, "MOS Field-Effect Transistors and Integrated Circuit," 1st ed., New York: A Wiley-Interscience publication, 1973, pp. 94-96.
[28] M. Kimira, Y. Kamada, S. Fujita, T. Hiramatsu, T. Matsuda, M. Furuta, and T. Hirao, "Mechanism analysis of photoleakage current in ZnO thin-film transistors using device simulation," Appl. Phys. Lett., Vol. 97, pp. 163503, 2010.
[29] B. G. Streetman, "Solid State Electronic Devices," 6th ed., New York: Prentice Hall International Inc., 1990, pp. 144.
[30] K. C. Kao, and W. Hwang, "Electrical Transport in Solid," 1st ed., New York: Pergamon Press Inc., 1981, pp. 146.

Tae-Young Ma He received Ph. D. degree in electronic engineering from Kyoungpook National University, Korea, in 1985. In 1987, he joined the Faculty of Gyeongsang National University, Jinju, Korea, where he currently is a professor of electrical engineering. His research interests are TTFT, Sensors etc.